The cultivation of human retinal pigment epithelial cells on *Bombyx mori* silk fibroin

Audra M. A. Shadforth [a], Karina A. George [a,b,c], Anthony S. Kwan [a,e], Traian V. Chirila [a,e,f,g], Damien G. Harkin [a,b,c,*]

[a] *Queensland Eye Institute, 41 Annerley Road, South Brisbane, Queensland 4101, Australia*

[b] *Discipline of Medical Sciences, Faculty of Science & Technology, Queensland University of Technology, Brisbane, Queensland 4001, Australia*

[c] *Institute of Health and Biomedical Innovation, Queensland University of Technology, Kelvin Grove, Queensland 4059, Australia*

[e] *Faculty of Health Sciences, University of Queensland, Herston, Queensland 4006, Australia*

[f] *Australian Institute for Bioengineering and Nanotechnology, University of Queensland, St. Lucia, Queensland 4072, Australia*

[g] *Discipline of Chemistry, Faculty of Science & Technology, Queensland University of Technology, Brisbane, Queensland 4001, Australia*

---

*Corresponding author (current address).

School of Biomedical Sciences, Faculty of Health, Queensland University of Technology, 2 George Street, Brisbane, Queensland 4001, Australia.

Tel: +61 7 3138 2552

Fax: +61 7 3138 6030

E-mail Address: d.harkin@qut.edu.au

Abstract

We have presently evaluated membranes prepared from *Bombyx mori* silk fibroin (BMSF), for their potential use as a prosthetic Bruch's membrane and carrier substrate for human retinal pigment epithelial (RPE) cell transplantation. Porous BMSF membranes measuring 3 μm in thickness were prepared from aqueous solutions (3% w/v) containing poly(ethylene oxide) (0.09%). The permeability coefficient for membranes was between 3 and 9×10^{-5} cm/s by using Allura red or 70 kDa FITC-dextran respectively. Average pore size (± sd) was 4.9 ± 2.3 μm and 2.9 ± 1.5 μm for upper and lower membrane surfaces respectively. Optimal attachment of ARPE-19 cells to BMSF membrane was achieved by pre-coating with vitronectin (1 μg/mL). ARPE-19 cultures maintained in low serum on BMSF membranes for approximately 8 weeks, developed a cobble-stoned morphology accompanied by a cortical distribution of F-actin and ZO-1. Similar results were obtained using primary cultures of human RPE cells, but cultures took noticeably longer to establish on BMSF compared with tissue culture plastic. These findings encourage further studies of BMSF as a substrate for RPE cell transplantation.

Keywords:

Silk fibroin

Retinal pigment epithelium

Bruch's membrane

Age-related macular degeneration

Transplantation

Abbreviated running title:

Retinal pigment epithelium grown on silk fibroin

1. Introduction

Silk extracted from the cocoons of the domesticated silkworm *Bombyx mori* has been used in the manufacture of surgical sutures and more recently has been utilised as a source of materials for tissue engineering applications [1, 2]. In particular, fibroin, a fibrous protein responsible for the mechanical properties of silk fibers, can be readily purified and fashioned into a variety of structures that support the attachment and growth of numerous cell types of both epithelial as well as mesenchymal lineage. Its versatility has lead to this protein being considered as a biomaterial for reconstructing tissues found within the human eye [3]. Transparent membranes cast from aqueous solutions of silk fibroin have been successfully used as a substrate for corneal epithelial cells [4-7], corneal fibroblasts [8, 9] and corneal endothelial cells [10]. The resulting phenotype of corneal cell cultures grown on fibroin membranes suggests that they may prove useful in restoring transparency and barrier function to the ocular surface [4]. This success has led us to investigate whether fibroin might also prove suitable as a biomaterial for reconstructing other ocular tissues and especially the retinal pigment epithelium.

The retinal pigment epithelium, or RPE, is a highly specialised monolayer of epithelial cells that supports the survival and function of photoreceptor cells through a variety of structural features and metabolic activities [11]. One of the key structural features of the RPE is the maintenance of tight epithelial cell junctions that restrict the movement of solutes between the retina and an adjacent, highly vascularised tissue known as the choroid. Movement of solutes is further impeded by a dense layer of extracellular matrix known as Bruch's membrane that incorporates RPE's basement membrane [12]. The RPE, assisted by Bruch's membrane, regulates the movement of nutrients and waste products between the outer retina and choroidal blood supply via specialised trans-epithelial transport functions.

A healthy RPE together with a normal Bruch's membrane are, not surprisingly, essential for maintaining the function of photoreceptor cells, and thus vision, throughout adult life. Nevertheless, Bruch's membrane undergoes a variety of biochemical and structural changes with age [12] that, in conjunction with loss of adjacent RPE cells, leads to age-related macular degeneration (AMD), the leading cause of blindness in developed countries [13]. While the underlying causes of AMD are complex, the final pathological changes often include loss of RPE cells and underlying choroid tissue. Therefore it is logical to consider one form of potential treatment is the transplantation of RPE cells associated with some form of prosthetic Bruch's membrane [14]. Ideally, materials used in construction of the prosthetic Bruch's membrane might also be used as a carrier for the transplanted RPE cells. A key challenge in this field of research is therefore to identify materials that support the fabrication of an RPE carrier substrate, while also displaying a level of permeability that is at least equal to that of Bruch's membrane.

In the present study we report critical data on the attachment, growth and morphology of human RPE cells grown on membranes prepared from *Bombyx mori* silk fibroin (BMSF). In considering the importance of nutrient/waste exchange across the RPE/Bruch's membrane complex *in vivo,* we have utilised ultra-thin BMSF membranes measuring only a few microns in thickness. Permeability has been evaluated using membranes that have been rendered porous by casting BMSF in the presence low concentrations of poly(ethylene oxide) (PEO) which is later leached from the membrane by washing in water. Given that corneal cell attachment to BMSF is often improved in the presence of exogenous cell adhesion factors [8, 10], we have examined the effect of ECM proteins found naturally within the retina and RPE-basement membrane on RPE cell attachment to BMSF. We have initially conducted our studies using the spontaneously immortalised human RPE cell line ARPE-19 since this is a well-established model for human RPE cell function *in vitro* [15]. These studies include

morphological assessments of long-term ARPE-19 cultures (2 months) which are necessary to develop key morphological characteristics similar to those found *in vivo* including formation of tight junctional complexes and extension of microvilli from the apical surface. Finally, we report on the relative feasibility of establishing primary cultures of adult human RPE cells on BMSF compared with conventional tissue culture plastic.

2. Materials and methods

2.1. Materials

Bombyx mori cocoons were supplied by Tajima Shoji Co. Ltd. (Yokohama, Japan) with the pupae already removed. All chemical reagents were purchased from Sigma-Aldrich (St. Louis, MO, USA) and were of A.R. grade unless otherwise indicated. Tissue culture reagents were purchased from Invitrogen (Carlsbad, CA, USA) and the tissue culture plastic plates and flasks were Iwaki brand (Asahi Glass Co. Ltd. Japan) unless otherwise indicated.

2.2. Preparation of ultra-thin porous BMSF membranes

Aqueous solutions of BMSF were prepared as described previously [4, 6, 10]. Ultra-thin porous BMSF membranes were produced on a custom-built film-casting table. This apparatus consisted of an optically flat glass surface and an automated doctor blade that moves across the table. The height of the blade above the glass surface was set at 0.35 mm and a 12 % solution of a cyclic olefin copolymer (Topas® 80075-04; Topas Advanced Polymers, Germany) in cyclohexane was cast onto the glass sheet and dried overnight. An aqueous solution of 3% w/v BMSF containing 0.09% w/v PEO (MW ~ 900,000 g/mol) was then cast onto the copolymer film and covered with a perforated lid to slowly evaporate water

from the solution over 3 days. The membranes were subsequently removed from the casting table as a bilayered laminate. For structural stabilisation, β-sheet formation was induced by water annealing the membranes in a vacuum oven at -80 kPa with ~100 mL water for 6 hours. The BMSF membrane was delaminated from the Topas® film prior to use.

Discs of BMSF membrane were punched out and set up in our custom-made cell culture chambers manufactured from polytetrafluoroethylene (Teflon®) (Fig. 1). The BMSF was sterilised in 70 % ethanol for 20 min and then transferred to sterile Milli-Q water for 48 hours (with one change of water after 24 hours) to leach the PEO from the membranes.

2.3. Characterisation of membrane structure

The morphology of BMSF membranes was assessed by scanning electron microscopy using an FEI Quanta 200 SEM/ESEM microscope operating in standard high vacuum mode, with a standard tungsten cathode filament. Images were taken at 25 kV. Samples were placed on a specimen stub lined with double-sided adhesive, conducting tape then coated with a thin layer of carbon to reduce sample charging. Quantitative image analysis was performed using Image J (version 1.42) to determine pore sizes and membrane thickness from the SEM images.

2.4. Permeability of BMSF membranes

A horizontal diffusion cell was used to determine the permeability of the BMSF membranes to 3 model molecules: Allura red (496.42 Da), and two dextran molecules functionalised with fluorescein isothiocyanate, FITC-dextran 10kDa (average dextran molecular weight: 10,000 Da, approximate Stokes' radius of 23 Å) and FITC-dextran 70kDa

(average dextran molecular weight: 70,000 Da, approximate Stokes' radius of 60 Å). The chamber consisted of two stirred reservoirs connected by a 19-mm diameter tube containing 100 mL of ~ 0.5 μg/mL of the test molecule in PBS buffer in one reservoir and only PBS buffer in the other. The BMSF membranes or reference membranes were held between two o-rings separating the two reservoirs. Samples of 100 μL each were taken periodically from the PBS buffer reservoir and placed in a 96-well tissue culture plate. The concentration of the model molecules in these samples was determined using a Beckman Coulter Paradigm microplate spectrophotometer. Standards of appropriate concentration were prepared for each molecule to generate standard curves. Absorbance was measured at 504 nm for Allura red. For the FITC-dextran molecules, fluorescence emitted at 535 nm was measured using an excitation wavelength of 485 nm. Permeability coefficients were determined according to Eq. 1 using only data that displayed a linear rate of permeability through the membranes and the concentration of molecule in the buffer reservoir did not exceed 0.05 μg/mL.

$$P = \frac{dQ}{dt} \times \frac{1}{AC_a} \qquad \text{Eq. 1}$$

where P is the permeability coefficient (cm/s), dQ/dt is the penetration rate of the molecule (μg/s), A is the surface area of the membrane (cm^2) and C_a is the concentration of model molecule in the reservoir that had the model molecule added to it at the start of the experiment (~0.5 μg/mL). This equation is only valid when C_a is much greater than the concentration of model molecule in the receiving reservoir.

The permeability experiments were performed in triplicate at room temperature and reported as the average ± standard deviation (n=3) for each membrane. To ensure that there was not leakage of the molecules around the membranes, the chamber was tested using a

polyethylene membrane as the separating membrane. No permeability of Allura red was observed over 3 weeks, showing also that no leakage occurred around the o-rings holding the membranes in place.

2.5. Coating of BMSF membranes with ECM proteins

The potential enhancement of RPE cell attachment on BMSF was tested with pre-coating of ECM proteins onto the BMSF. The ultra-thin porous BMSF membrane, set up in the Teflon® chambers were coated overnight with recommended concentrations of ECM proteins according to manufacturer's instructions; 23.95 µg/mL laminin (Sigma Aldrich), 6.66 µg/mL fibronectin (Sigma Aldrich), 1 µg/mL vitronectin (Promega Corporation, Madison, WI) and 40 µg/mL collagen IV (Sigma Aldrich). Non-coated BMSF membranes were used as controls.

2.6. Routine culture of the ARPE-19 cells

The ARPE-19 cell line [15] (ATCC Cat No. CRL-2302) was routinely maintained in 75 cm^2 cell culture flasks in a 1:1 mixture of Dulbecco's modified Eagle's medium and Ham's F12 medium (DMEM/F12), supplemented with 1.2 g/L sodium bicarbonate, 2.5 mM L-glutamate, 15 mM HEPES, 0.5 mM sodium pyruvate, 10% foetal bovine serum (FBS) and 1% antibiotic/antimycotic solution.

2.7. Assessment of RPE cell attachment to BMSF membranes

Approximately 80,000 ARPE-19 cells were seeded in serum-free culture medium (as above for routine culture, but without FBS) onto ECM-coated BMSF membranes or tissue culture plastic. Cells seeded into tissue culture plastic wells in culture medium supplemented with 10% FBS was used as a positive control (TCP + FBS). After 4 hours incubation (37 °C,

5% CO_2) the cultures were washed with Hank's Buffered Salt Solution (HBSS) and the DNA content of the attached cells was quantified using a PicoGreen assay as reported by Lawrence *et al.* [9]. Differences in our method involved each sample being incubated at room temperature in 1 mL of 0.1% Triton X-100 in a TE buffer (10 mM Tris, 2 mM EDTA, pH 8.0) for 30 minutes, and Lambda phage DNA (Invitrogen, Life Technologies, Mulgrave, Australia) was used at concentrations of 0, 0.025, 0.25, 1, 2.5 and 10 ng/mL to generate a standard curve. The experiment was performed in triplicate and repeated three times. Statistical differences between BMSF membranes alone and ECM-coated BMSF membranes were determined using a one-way analysis of variance (n = 3, using mean values for each triplicate).

2.8. Establishment and maintenance of long-term ARPE-19 cultures on BMSF membrane

Two test materials were used for the RPE long-term culture experiments: ultra-thin porous BMSF membrane set up in the Teflon® chambers and tissue culture plastic (24-well tissue culture plates). Based upon results from Fig. 3, each culture substrate was pre-coated with 1 μg/mL vitronectin and seeded with ARPE-19 cells at a density of 10,000 cells per cm^2. Cultures were initially grown to confluency in DMEM/F12 supplemented with 10% v/v FBS and 1% antibiotic/antimycotic, then maintained for an additional 7 weeks in a reduced serum content of 1% with feeding once per week.

2.9. Immunocytochemistry

Cultures were fixed in 3.7% buffered formalin, blocked in 2% normal goat serum in PBS, permeabilised with 0.1% Triton X-100 in 100 mM HEPES buffer (pH 7.2), and stained with rhodamine phalloidin, Hoechst nuclear dye and an antibody to ZO-1 (Clone Zo1-1A12,

1:100 dilution). The secondary antibody used was an Alexa 488-conjugated goat-anti mouse IgG (Molecular Probes).

2.10. Isolation and cultivation of primary human RPE

Human posterior eye cups were obtained from the Queensland Eye Bank (Princess Alexandra Hospital, Brisbane, Australia) and used with ethics approval and donor consent. The dissection and isolation method used was a modified combination of methods previously published by Sonoda *et al.* [16] and Engelmann and Valtink [17]. The eye cup is dissected flat into four quadrants using the optic disc as the central point. The vitreous is usually removed with the force of the incisions and the sensory retina is carefully peeled away. The exposed RPE-choroid layer from each quadrant is gently stripped from the underlying sclera. Each sheet of RPE-choroid is incubated in 500 µL collagenase IA and collagenase IV solution (0.5 mg/mL of each) and incubated at 37°C for 40 minutes. The collagenase activity is stopped by adding 1 mL HBSS, and each pigmented sheet is gently shaken to release the RPE cells. These can come off as individual cells or sheets of RPE. The RPE cell solution is gently pelleted at 10*g* for 5 minutes. The pellet is resuspended and seeded onto ultra-thin porous BMSF membrane set up in the Teflon® chambers pre-coated with 1 µg/mL vitronectin (Promega Corporation, Madison, WI, USA). Cultures were grown in DMEM/F12 supplemented with 10% FBS v/v, 1% Insulin-Transferrin-Selenium and 1% antibiotic-antimycotic, and were fed three times per week.

3. Results

3.1. Characterisation of BMSF membranes used for RPE cells.

We have previously demonstrated that 10-20 μm thick membranes prepared from BMSF support the growth of corneolimbal epithelial cells [4], but in considering the more intensive transport functions of the RPE we chose to presently evaluate ultra-thin (~3 μm thick) membranes which additionally contained pores generated through casting in the presence of PEO. The resulting membranes appeared slightly opaque when held to light but were sufficiently transparent to enable direct observations of cell growth (Fig. 1). Moreover, the membranes were strong enough to support handling with forceps and remained intact during mounting within Teflon® cell culture chambers (Fig. 1). Examination of resulting membranes by SEM confirmed the presence of pore-like structures of variable size (Fig. 2). Significant differences in pore size distribution were observed between the upper membrane surface (exposed to air during drying) and the lower membrane surface which had been exposed to the Topas® coated casting table during drying (Fig. 2d). The average pore sizes were 4.9 ± 2.3 μm (mean ± sd, N = 287) and 2.9 ± 1.5 μm (N = 493) for upper and lower surfaces respectively. While examination of membranes in cross-section confirmed that some pores traversed the width of the structure, the number of true pores remained difficult to determine based upon flat views of representative samples for each side of the membrane. The level of permeability was therefore assessed by measuring diffusion of coloured (Allura red) or fluorescently labelled molecules (FITC-dextran 10kDa and 70kDa). Porous track-etched membranes (14 μm track etched pores in polycarbonate) and non-porous polyethylene membranes were used as positive and negative controls respectively (data not shown). The resulting analysis (Fig. 2e) confirmed that the porous BMSF membranes were permeable to all solutes tested with permeability coefficients ranging approximately between 3 and 9×10^{-5}

cm/s. A trend towards faster diffusion of Allura red was observed, but this was not found to be statistically significant.

3.2. Effect of ECM proteins of ARPE-19 cell attachment to BMSF membranes.

Non-treated BMSF membranes were inherently less adhesive for ARPE-19 cells than regular tissue culture plastic (with or without serum in culture medium). While trends towards increased cell attachment were observed using membranes that had been pre-coated with either serum-supplemented culture medium, laminin, vitronectin or collagen IV, only vitronectin-treated membranes generated significant results ($p<0.05$) which were similar to that supported by tissue culture plastic (Fig. 3). Fibronectin had no noticeable effect.

3.3. Evaluation of long-term ARPE-19 cultures grown on BMSF membranes.

While the ARPE-19 cell line is widely used as a model of human RPE cell function, long-term culture in the presence of reduced serum levels are required in order to induce the development of an epithelial morphology closer to that required for functioning RPE cells *in vivo* [18]. A key example is tight junction formation which can be studied through immunostaining for ZO-1 and changes can be observed in the distribution of F-actin filaments through a reduction in stress fibres and relocation to the cell-cell boundaries. As shown in Fig. 4, similar distribution patterns for both ZO-1 and F-actin were observed for long-term cultures (8 weeks) grown on either tissue culture plastic or BMSF. While some cells retained prominent stress fibres and displayed a diffuse staining pattern for ZO-1, the majority of cells cultured on either material displayed a peripheral arrangement of both markers. The more epithelial areas within cultures likewise correlated with the presence of cell surface projections of similar size and shape to microvilli which are observed on the apical surface of RPE cells *in vivo* and serve a critical role in trans-epithelial transport.

3.4. Establishment of primary human RPE cultures on BMSF membranes.

Unlike other epithelial tissues, the adult RPE generally displays poor evidence of growth *in vitro*, but successful cultures can often be achieved through the use of younger donors or tissue that has only been stored for a few days post-mortem. Most cultures initially grew slowly and retained melanin pigment, but with time developed islands of less-pigmented cells with a lower cytoplasmic-to-nuclear ratio consistent with a faster rate of proliferation and a similar appearance to those displayed in Fig. 5b. Cultures did not respond well to passaging and often displayed evidence of a more fibroblastic morphology. In general, a similar pattern of growth was observed on the BMSF membranes coated with vitronectin, however, growth was substantially poorer compared to that observed on tissue culture plastic. Moreover, successful cultures on BMSF displayed noticeably fewer cells when compared in parallel to those grown on tissue culture plastic (compare Fig. 5a and b). Given sufficient time, however, a number of more proliferative cultures were achieved on BMSF after 8 weeks growth (Fig. 5c). Staining of these cultures for F-actin and ZO-1 revealed evidence of tight junctions similar to that developed in long-term ARPE-19 cultures. Many cells retained melanin pigment as demonstrated both phase contrast microscopy and autofluorescence (Fig. 5d).

4. Discussion

Silk fibroin has significant potential as a biomaterial owing to a relatively unique combination of physical and chemical properties [1]. We and other groups have recently established that these properties can be exploited for the purpose of generating corneal tissue equivalents [4, 6, 7, 9, 10]. Our present findings demonstrate that BMSF supports cultivation of retinal pigment epithelial (RPE) cells and might therefore provide a useful material to

construct RPE tissue equivalents for the treatment of AMD. In doing so, however, BMSF joins a growing list of other materials with similar potential [19, 20] and so careful consideration must be given to the question of what makes BMSF a worthy candidate for further study from within a pool of potential options.

While many materials, both natural and synthetic, support the attachment and growth of RPE cells [19, 20], the material must also support adequate movement of nutrients and waste products to at least an equal level as that observed across Bruch's membrane. It is thus significant that the membranes produced from BMSF presently are of similar thickness to Bruch's membrane (approximately 3 μm) and are approximately four-fold more permeable (based upon permeability coefficient for dextrans) [21]. By comparison, the permeability coefficient for dextran through collagen membranes, of similar thickness to those used presently, has been reported as 10,000-fold less [22] than for values attained using Bruch's membrane [21]. The permeability of BMSF membranes used presently is undoubtedly assisted by the presence of pores although we have shown recently elsewhere [4] that non-porous BMSF membranes that were approximately twice as thick as those used presently, remain permeable with a permeability coefficient for dextran which is approximately half of that for the porous membranes. We can therefore surmise that neither porous nor non-porous BMSF membranes would affect adversely the permeability characteristics of the outer blood retinal barrier.

The ability of BMSF to support cell attachment and growth is a curious phenomenon since the peptide sequences of BMSF contain little evidence of recognizable cell-adhesion motifs. Thus the principal mechanism of cell attachment to BMSF is most likely mediated *via* an intermediary such as serum proteins absorbed from the culture medium including vitronectin and fibronectin. We therefore chose in the present study to optimise the attachment of RPE cells to BMSF membranes by pre-coating with a variety of extracellular

matrix proteins including vitronectin, which in addition to being present in serum [23], is produced by photoreceptors and RPE cells [24], and is present within Bruch's membrane [25]. Moreover, RPE cells express integrin receptors for vitronectin [26]. It is therefore not surprising that our best results in cell attachment assays were achieved using vitronectin-coated membranes and on this basis we chose to use vitronectin-coated membranes in long-term cultures with ARPE-19 cells and primary cultures of human RPE cells. Vitronectin is naturally a very adherent protein and as such many other materials apart from BMSF may well be rendered suitable for RPE culture. It should be noted, however, that the proteinaceous nature of BMSF does provide opportunities for more sophisticated approaches if required owing to the abundance of reactive side groups including amines. In this sense, BMSF along with other proteins including collagen, might perhaps be more easily "tuned" to the requirements of RPE cells if required.

In addition to supporting RPE attachment and growth, any material to be used as a substrate for RPE transplantation must ultimately support the adoption of a fully differentiated and functional RPE monolayer. One of the key features of RPE differentiation and function is the development of a tightly cobblestoned morphology as indicated through a peripheral distribution of F-actin fibers. Moreover, this cytoskeletal arrangement is commensurate with the development of tight cell-cell junctions as often illustrated through staining for the zonula occludens protein ZO-1. The ARPE-19 cell line does not naturally display this morphology during routine culture but can be encouraged to do so when cultured for extended periods in culture medium containing reduced levels of serum [18]. It is thus encouraging that long-term cultures established on BMSF membranes retained this developmental potential and also produced cellular extensions which resemble the size and shape of microvilli observed on the apical surface of RPE cells *in vivo.*

While ARPE-19 cells are highly regarded as a model system for RPE studies, clinical applications will ultimately require the use of primary RPE cells isolated from either autologous or donor tissue. We therefore completed our study by performing a preliminary assessment of primary RPE cell growth on BMSF membranes. While the variable performance of primary cultures makes it difficult to perform a more quantitative analysis, the morphology of resulting cultures is consistent with those grown on other materials including tissue culture plastic and encourages further studies. In particular, the noticeably slower growth of primary RPE cultures on vitronectin-coated-BMSF compared with tissue culture plastic, suggests that further "tuning" of the substrate surface will be required for optimisation.

Conclusion

The thickness and permeability of BMSF membranes used in this study are consistent with the requirements of a prosthetic Bruch's membrane. Moreover, our findings confirm the feasibility of growing RPE cells on these BMSF membranes. This is an important finding, as an ideal material for constructing a prosthetic Bruch's membrane with attached RPE cells has yet to be found. BMSF is therefore a worthy candidate for exploration as a vehicle for RPE transplantation in pre-clinical trials of AMD treatment.

Acknowledgements

This work was supported by a grant received from Vision Australia administered through the Ophthalmic Research Institute of Australia (awarded to ASK, TVC and DGH) with supplementary funding from the National Health & Medical Research Council of Australia (awarded to DHG and TVC) and the Prevent Blindness Foundation, Queensland,

Australia (supported through Viertel's Vision program). We also acknowledge the support of staff from the Queensland Eye Bank for facilitating access to donor eye used in this study.

References

1. Altman GH, Diaz F, Jakuba C, Calabro T, Horan RL, Chen J, et al. Silk-based biomaterials. Biomaterials 2003;24:401-16.
2. Wang Y, Kim HJ, Vunjak-Novakovic G, Kaplan DL. Stem cell-based tissue engineering with silk biomaterials. Biomaterials 2006;27:6064-82.
3. Harkin DG, George KA, Madden PW, Schwab IR, Hutmacher DW, Chirila TV. Silk fibroin in ocular tissue reconstruction. Biomaterials 2011;32:2445-58.
4. Bray LJ, George KA, Ainscough SL, Hutmacher DW, Chirila TV, Harkin DG. Human corneal epithelial equivalents constructed on Bombyx mori silk fibroin membranes. Biomaterials 2011;32:5086-91.
5. Chirila T, Barnard Z, Zainuddin, Harkin D. Silk as a substratum for cell attachment and proliferation. Materials Science Forum 2007;561-565:1549-52.
6. Chirila TV, Barnard Z, Zainuddin, Harkin DG, Schwab IR, Hirst LW. *Bombyx mori* silk fibroin membranes as potential substrata for epithelial constructs used in the management of ocular surface disorders. Tissue Eng Part A 2008;14:1203-11.
7. Higa K, Takeshima N, Moro F, Kawakita T, Kawashima M, Demura M, et al. Porous Silk fibroin film as a transparent carrier for cultivated corneal epithelial sheets. J Biomater Sci Polym Ed 2010; in press.
8. Gil ES, Mandal BB, Park SH, Marchant JK, Omenetto FG, Kaplan DL. Helicoidal multi-lamellar features of RGD-functionalized silk biomaterials for corneal tissue engineering. Biomaterials 2010;31:8953-63.
9. Lawrence BD, Marchant JK, Pindrus MA, Omenetto FG, Kaplan DL. Silk film biomaterials for cornea tissue engineering. Biomaterials 2009;30:1299-308.

10. Madden PW, Lai JNX, George KA, Giovenco T, Harkin DG, Chirila TV. Human corneal endothelial cell growth on a silk fibroin membrane. Biomaterials 2011;32:4076-84.

11. Strauss O. The retinal pigment epithelium in visual function. Physiol Rev 2005;85:845-81.

12. Booij JC, Baas DC, Beisekeeva J, Gorgels TG, Bergen AA. The dynamic nature of Bruch's membrane. Prog Retin Eye Res 2010;29:1-18.

13. de Jong PT. Age-related macular degeneration. N Engl J Med 2006;355:1474-85.

14. Binder S, Stanzel BV, Krebs I, Glittenberg C. Transplantation of the RPE in AMD. Prog Retin Eye Res 2007;26:516-54.

15. Dunn KC, Aotaki-Keen AE, Putkey FR, Hjelmeland LM. ARPE-19, a human retinal pigment epithelial cell line with differentiated properties. Exp Eye Res 1996;62:155-69.

16. Sonoda S, Spee C, Barron E, Ryan SJ, Kannan R, Hinton DR. A protocol for the culture and differentiation of highly polarized human retinal pigment epithelial cells. Nat Protoc 2009;4:662-73.

17. Engelmann K, Valtink M. RPE cell cultivation. Graefes Arch Clin Exp Ophthalmol 2004;242:65-7.

18. Luo Y, Zhuo Y, Fukuhara M, Rizzolo LJ. Effects of culture conditions on heterogeneity and the apical junctional complex of the ARPE-19 cell line. Invest Ophthalmol Vis Sci 2006;47:3644-55.

19. Hynes SR, Lavik EB. A tissue-engineered approach towards retinal repair: scaffolds for cell transplantation to the subretinal space. Graefes Arch Clin Exp Ophthalmol 2010;248:763-78.

20. Kwan ASL, Chirila TV, Cheng S. Development of tissue-engineered membranes for the culture and transplantation of retinal pigment epithelial cells. In: Chirila TV, editor. Biomaterials and regenerative medicine in ophthalmology. Cambridge, UK: Woodhead Publishing Ltd, 2009. p. 390-408.

21. Hussain AA, Starita C, Hodgetts A, Marshall J. Macromolecular diffusion characteristics of ageing human Bruch's membrane: implications for age-related macular degeneration (AMD). Exp Eye Res 2010;90:703-10.

22. Lu JT, Lee CJ, Bent SF, Fishman HA, Sabelman EE. Thin collagen film scaffolds for retinal epithelial cell culture. Biomaterials 2007;28:1486-94.

23. Schvartz I, Seger D, Shaltiel S. Vitronectin. Int J Biochem Cell Biol 1999;31:539-44.

24. Ozaki S, Johnson LV, Mullins RF, Hageman GS, Anderson DH. The human retina and retinal pigment epithelium are abundant sources of vitronectin mRNA. Biochem Biophys Res Commun 1999;258:524-9.

25. Anderson DH, Hageman GS, Mullins RF, Neitz M, Neitz J, Ozaki S, et al. Vitronectin gene expression in the adult human retina. Invest Ophthalmol Vis Sci 1999;40:3305-15.

26. Nandrot EF, Anand M, Sircar M, Finnemann SC. Novel role for $\alpha_v\beta_5$-integrin in retinal adhesion and its diurnal peak. Am J Physiol Cell Physiol 2006;290:C1256-62.

Figure 1

Click here to download high resolution image

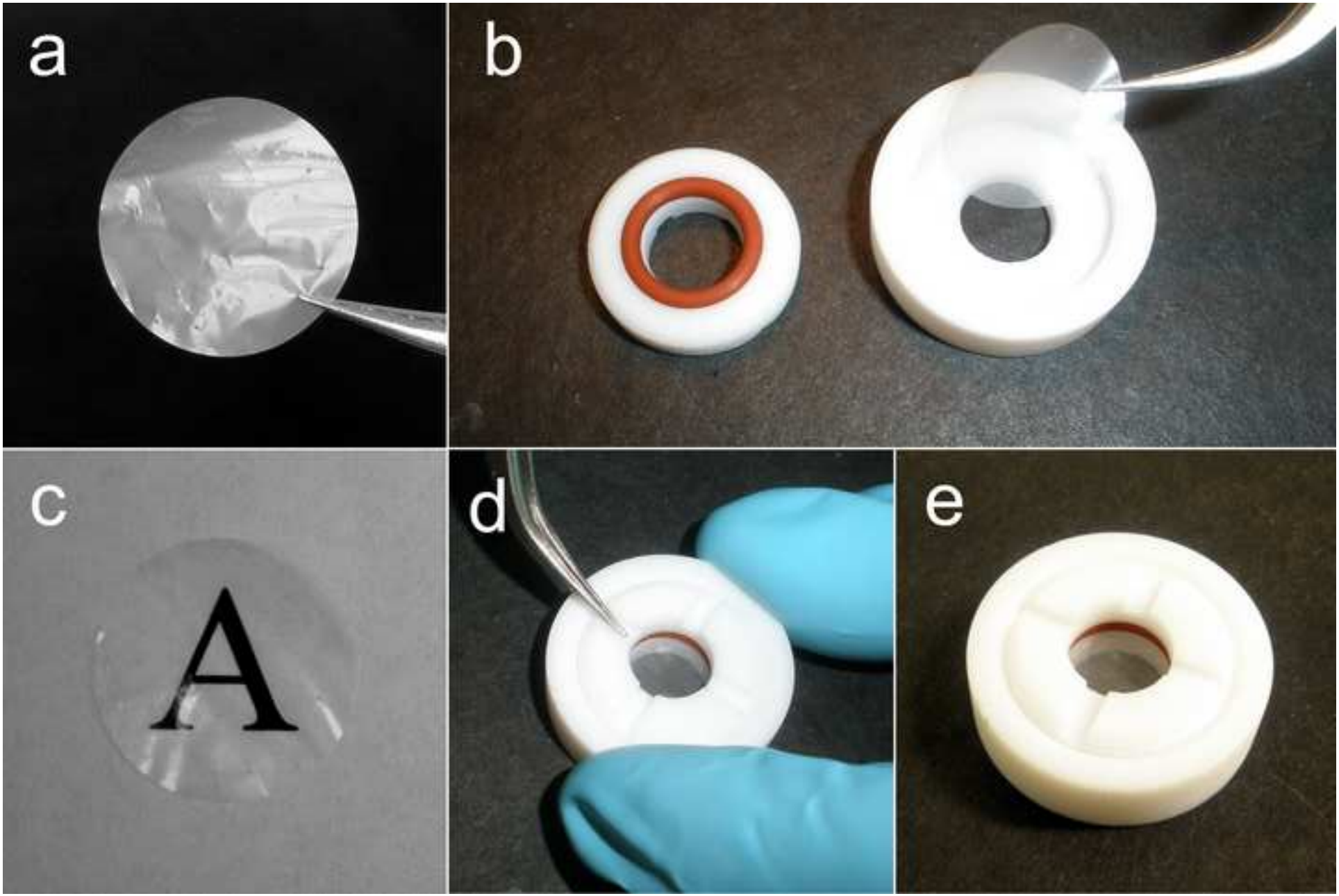

Figure 2

Click here to download high resolution image

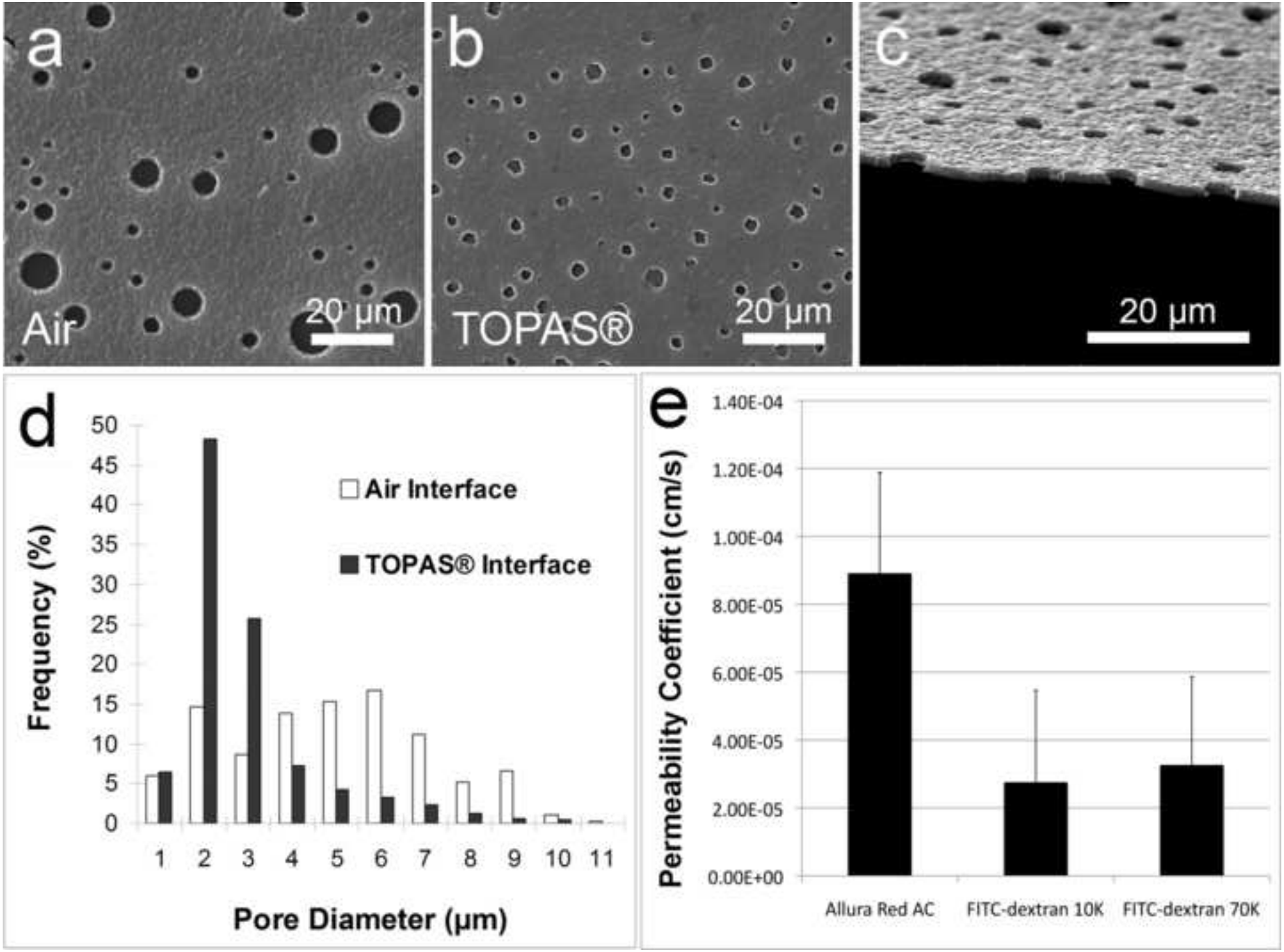

Figure 3

Click here to download high resolution image

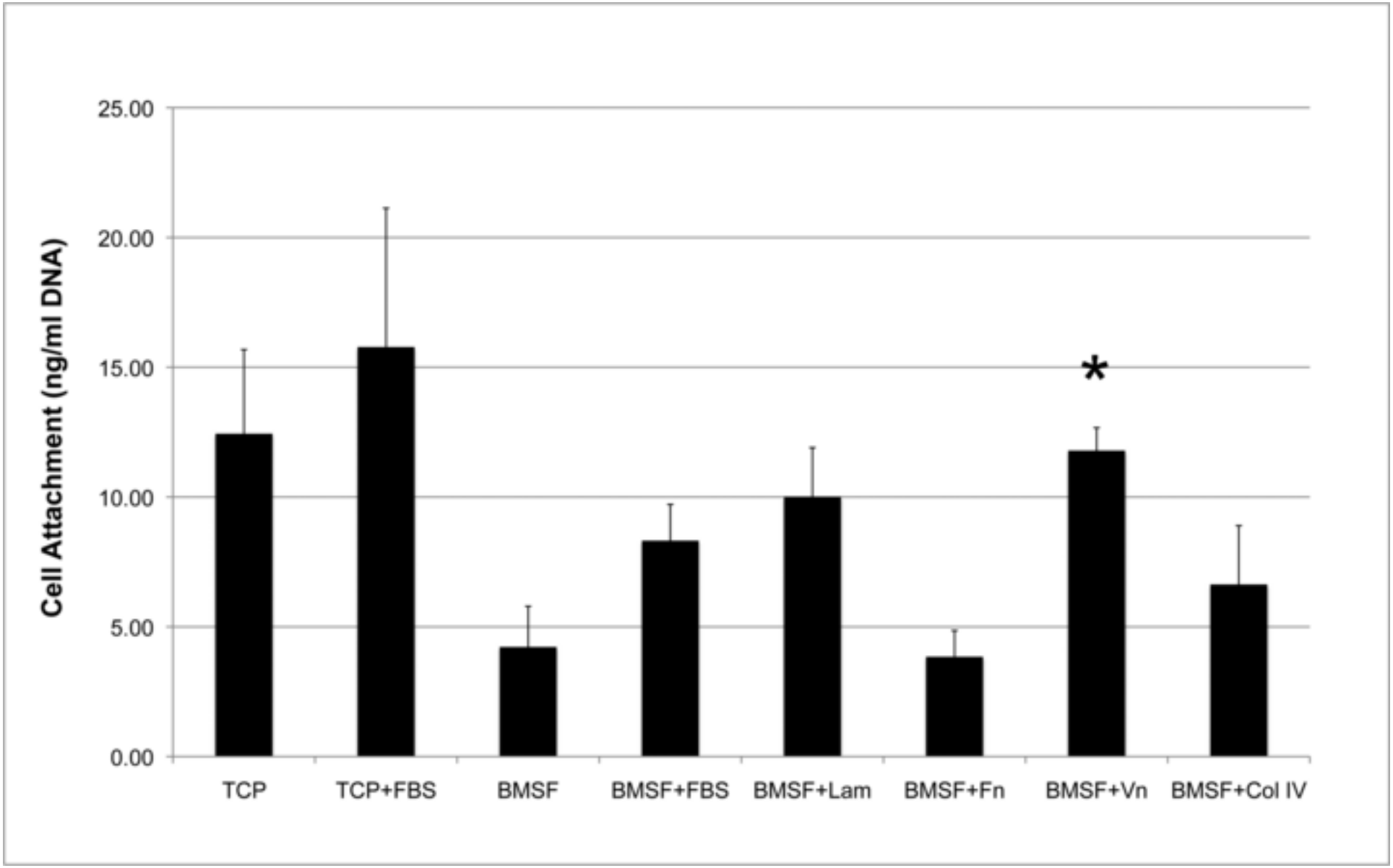

Figure 4
Click here to download high resolution image

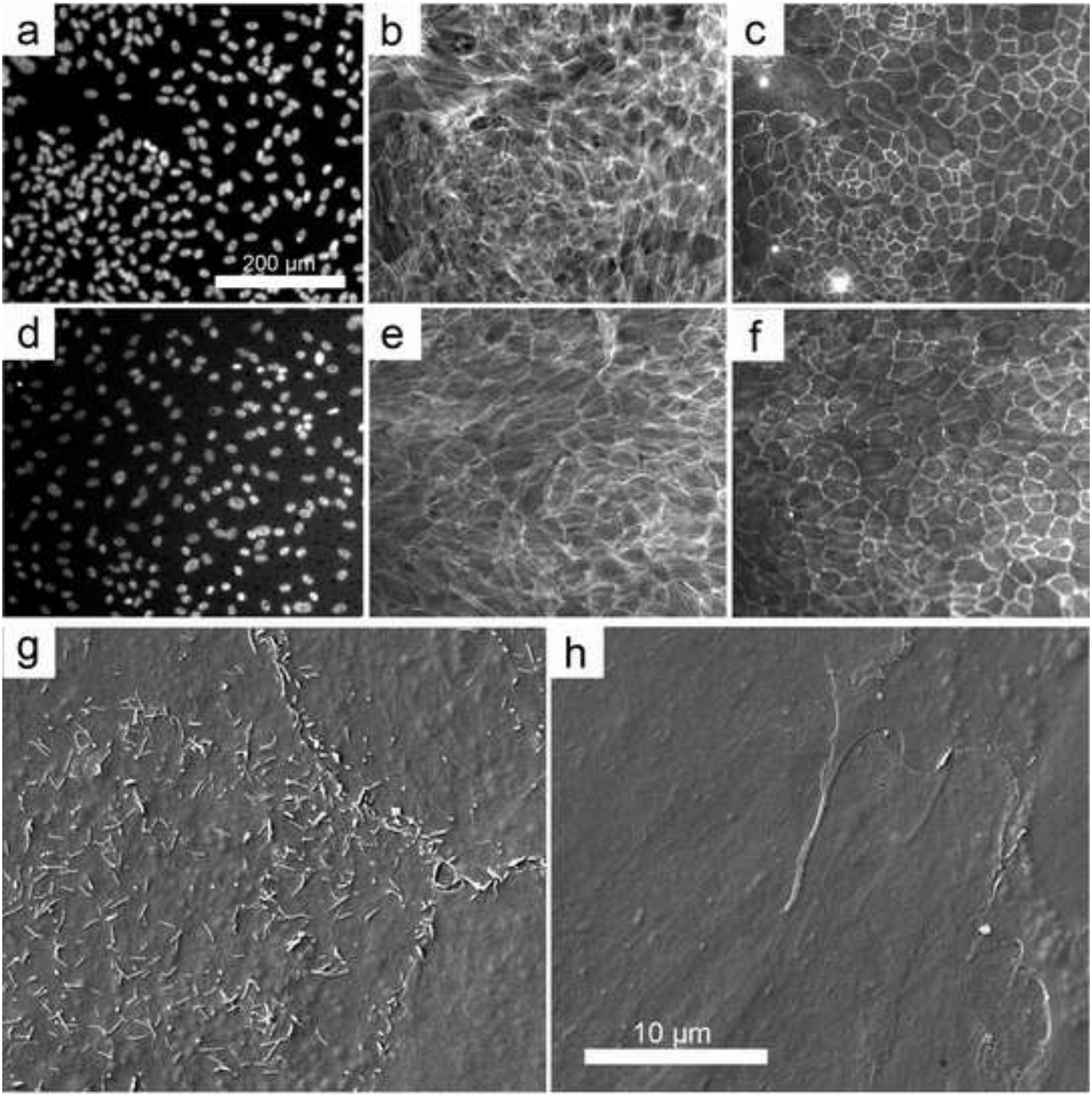

Figure 5

Click here to download high resolution image

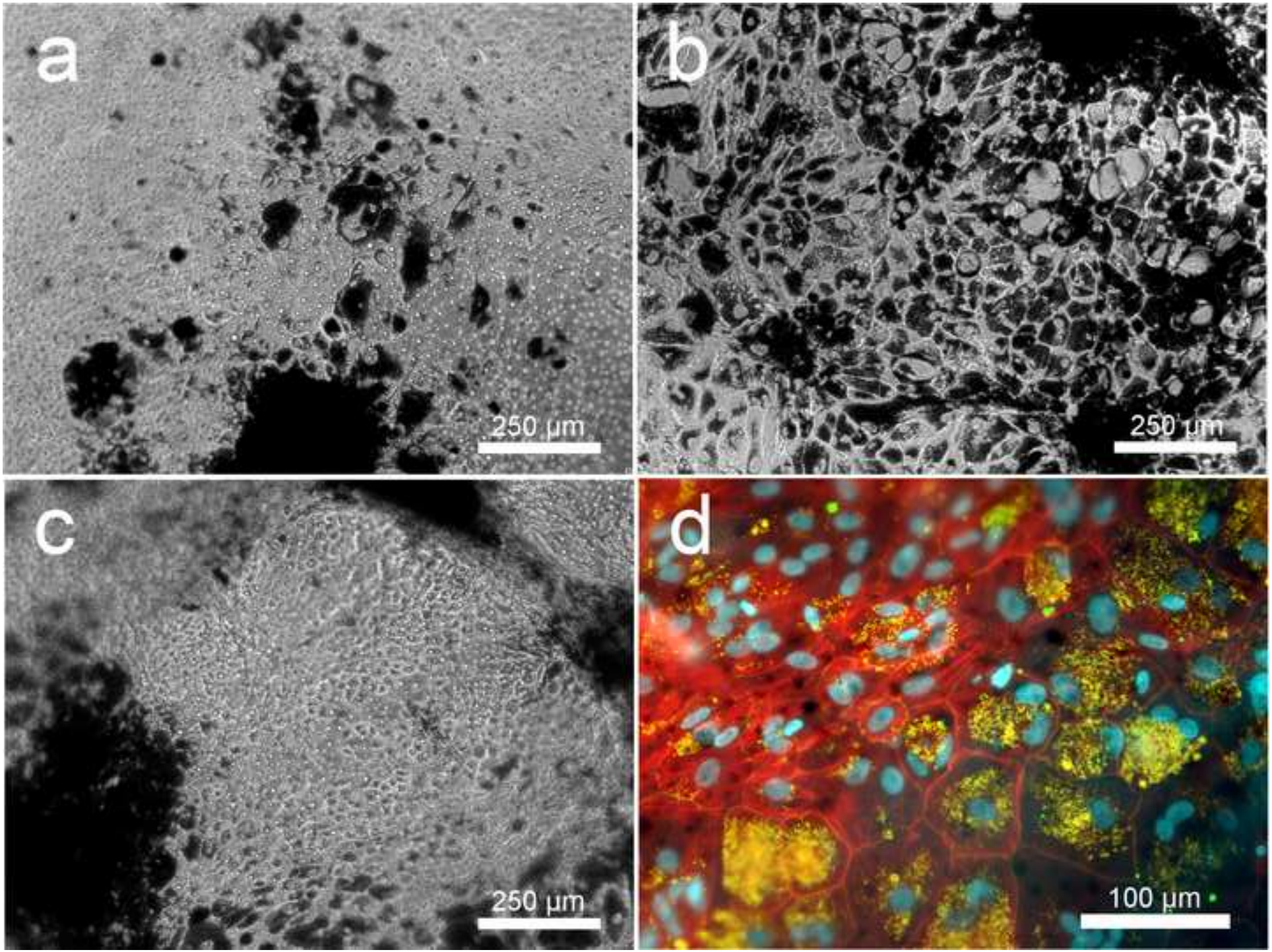

Figure Captions

Fig. 1. Appearance and assembly of BMSF membranes into cell-culture chamber.

(a and b) Appearance of BMSF membranes (35 mm discs) as photographed while being held up to light or placed above letter of printed text. (c-e) Stages of membrane assembly into custom-made cell culture chambers consisting of two inter-locking Teflon® rings and silicon o-ring. A locking mechanism is achieved by manufacturing the upper chamber piece to screw down into base.

Fig. 2. Ultrastructure and permeability of ultra-thin, porous BMSF membranes.

(a-c) Scanning electron microscopy images of BMSF membranes as viewed from above (air interface), below (Topas® interface), and side profile, respectively. (d) Histogram of pore size distribution as viewed from the upper (air interface) and lower (Topas® interface), respectively. (e) Relative permeability of BMSF membranes to Allura red AC (496 Da) and FITC-conjugated dextran (10 and 70 kDa).

Fig. 3. Optimisation of ARPE-19 cell attachment to BMSF membranes.

Attachment of ARPE-19 cells to BMSF and tissue culture plastic (TCP) was assessed after 4 hours via measurement of DNA content (PicoGreen assay). Cells seeded onto TCP in serum-supplemented medium was used as a positive control (TCP+FBS). Test samples consisted of non-treated membrane (BMSF) and membranes that had been pre-coated overnight with either serum-supplemented culture medium (BMSF+FBS), laminin (BMSF+Lam), fibronectin (BMSF+Fn), vitronectin (BMSF+Vn), or collagen IV (BMSF+Col IV). Asterisk denotes significant difference compared to non-treated BMSF membranes ($p<0.05$).

Fig. 4. Morphology of ARPE-19 cells following long-term cultivation on ultra-thing, porous BMSF membranes.

ARPE-19 cells were seeded (10,000 per cm^2) onto BMSF membranes pre-coated with vitronectin, grown to confluency in medium containing 10% foetal bovine serum (FBS), then grown for an additional 7 weeks in medium supplemented with 1% FBS. (a to c) ARPE-19 cells grown on tissue culture plastic. (d to f) ARPE-19 cells grown on ultra-thin porous BMSF membrane. (a and d) Nuclei revealed through staining with Hoechst dye. (b and e) F-actin fibres demonstrated by staining with rhodamine phalloidin. (c and f) Tight junction formation revealed through immunostaining for ZO-1. (g and h) Scanning electron microscopy of ARPE-19 cultures after 7 weeks growth on porous BMSF membranes. Cells within more cobble-stoned areas display apical projections resembling microvilli (g), whereas those retaining a more fibroblastic morphology display overlapping lamellipodial extensions (h).

Fig. 5. Establishment of primary human RPE cultures on ultra-thin, porous BMSF membranes.

Primary cultures of human RPE cells were established and grown for up to two months on tissue culture plastic (control) and vitronectin coated BMSF membranes. (a) Appearance of typical culture on BMSF after 1 month. (b) corresponding image of culture established on tissue culture plastic after 1 month. (c) Appearance of culture on BMSF after 2 months displaying island of smaller and less pigmented cells towards centre of field. (d) Higher power view of culture displayed in part ‘c’ after staining with rhodamine phalloidin for F-actin (red), Hoechst nuclear stain (blue) and immunostaining for ZO-1 (green). Co-localisation of ZO-1 at cell periphery with F-actin results in a yellow to orange colour. Melanin pigment appears bright yellow owing to autofluorescence across spectrum of filter sets used.